Global NOx Measurements in Turbulent Nitrogen-Diluted Hydrogen Jet Flames

N. Weiland[1] and P. Strakey[2]

[1]National Energy Technology Laboratory, Pittsburgh, Pennsylvania, 15236-0940, USA

[2] National Energy Technology Laboratory, Morgantown, West Virginia, 26507-0880, USA

Turbulent hydrogen diffusion flames diluted with nitrogen are currently being studied to assess their ability to achieve the DOE Turbine Program's aggressive emissions goal of 2 ppm NOx in a hydrogen-fueled IGCC gas turbine combustor. Since the unstrained adiabatic flame temperatures of these diluted flames are not low enough to eliminate thermal NOx formation, the focus of the current work is to study how the effects of flame residence time and global flame strain can be used to help achieve the stated NOx emissions goal. Dry NOx measurements are presented as a function of jet diameter, nitrogen dilution, and jet velocity for a turbulent hydrogen/nitrogen jet issuing from a thin-lipped tube in an atmospheric pressure combustor. The NOx emission indices from these experiments are normalized by the flame residence time to ascertain the effects of global flame strain and fuel Lewis Number on the NOx emissions. In addition, dilute hydrogen diffusion flame experiments were performed in a high-pressure combustor at 2, 4 and 8 atm. The NOx emission data from these experiments are discussed, as well as the results from one-dimensional flame calculations.

1. Introduction

One of the promising technologies being evaluated for carbon capture in coal-fired power plants by the U.S. Department of Energy (DOE) involves employing a water gas shift reaction to convert the syngas in an IGCC to a stream of hydrogen and carbon dioxide. After separation of the carbon dioxide for sequestration, a stream of high-purity hydrogen is available for combustion in the IGCC's gas turbine. In addition, nitrogen byproduct from the coal gasifier's air separation unit is available to dilute the hydrogen by about 50%, helping to control combustion temperatures in the gas turbine. These processes form the basis for the DOE's FutureGen Project, which endeavors to design and build a near-zero emissions research power plant by the year 2012.

One of the major technology barriers to applying current state-of-the-art dry low NOx, lean-premixed combustion to a hydrogen-base fuel is combustor flashback, which can result from the significantly higher flame-speed of hydrogen compared to natural gas. Due to this inherent difficulty with premixed combustion, the current generation of fielded gas turbines operating on hydrogen/nitrogen or syngas mixtures use a diffusion flame approach to combustion [1], thereby eliminating the potential for flashback problems. However, the NOx emissions from these combustors are in the range of 10-25 ppm, which are much higher than the DOE goal of 2 ppm NOx, corrected to 15% O2. Since there is little data available in the literature on diffusion flame combustion of hydrogen/nitrogen mixtures with air, the current study is focused on evaluating

the basic NOx emission characteristics of these flames, with the intent of providing information that will be useful in designing a dry, low-NOx hydrogen/nitrogen diffusion flame combustor.

The adiabatic flame temperature of a mixture of equal parts of hydrogen and nitrogen with stoichiometric air is about 2025 K, indicating that thermal NO is an important NOx formation pathway in these diffusion flames. One strategy for reducing thermal NOx is to reduce the residence time in the diffusion flame by increasing the jet velocity and/or reducing the jet diameter, though this also tends to increase flame strain and results in turbulence-chemistry interactions that promote NOx formation through the increase of super-equilibrium O-atom concentrations [2–4]. The effects of flame strain are more apparent when the NOx emission index is normalized by a characteristic flame residence time, $\tau_r = L_f^3/u_0 d_0^2$, where L_f is the flame length, u_0 is the jet exit velocity, and d_0 is the jet exit diameter. According to Chen and Driscoll [5], the normalized emission index scales as:

$$EINO_x \Big/ \left(L_f^3 \Big/ u_0 d_0^2\right) \propto Re^{m-1/2} Da^n \tag{1}$$

where Re is the Reynolds number at the jet exit and Da is the Damköhler number, which is inversely proportional to the global strain rate, u_0/d_0^*. The global strain rate can also be viewed as a characteristic mixing time, where the jet momentum diameter, $d_0^* = d_0(\rho_0/\rho_\infty)^{1/2}$, ρ_0 is the jet exit density, and ρ_∞ is the ambient air density.

In experiments with pure hydrogen and helium-diluted hydrogen [5, 6], the data is very well fit using $m = 1/2$ and $n = -1/2$ in Eq. (1). This well-known scaling relation has been verified by various modeling studies [3, 4, 7, 8], and shows that normalized NOx emissions increase with respect to flame strain due to turbulence-chemistry interactions that increase O-atom concentrations to higher super-equilibrium levels. In the absence of flame strain effects an equilibrium chemistry assumption should yield $n = 0$, however, subsequent studies by Chen and co-workers show that for hydrogen diluted by 60% argon or carbon dioxide, $n \approx 2/3$, meaning that flame strain helps reduce NOx emissions [9].

This result is attributed to low fuel Lewis number (Le_F), which is defined here as the ratio of the thermal diffusivity of the hydrogen/diluent mixture to the mass diffusivity of the hydrogen in the diluent. Values of Le_F for various dilution gases and levels of dilution are given in Table 1. Gabriel and co-workers hypothesize that the value of n increases as the fuel Lewis number decreases below 0.9 with increasing dilution of the hydrogen [9]. A secondary goal of the present study is to test this hypothesis, as increasing nitrogen dilution from 10% to 60% will decrease the fuel Lewis number from 1.66 to 0.68, the region in which n is predicted to exhibit a positive slope and flame strain and residence time effect are both expected to help reduce NOx emissions.

Table 1: Fuel Lewis number as a function of type and level of diluent in hydrogen [10]. Entries denoted by * were tested by Gabriel et. al. [9].

Diluent mole fraction	N_2	He	Ar	CO_2
0.1	1.661	0.994	1.626	1.830
0.2	1.387	0.998*	1.389*	1.438*
0.3	1.162	1.004	1.187	1.139
0.4	0.974	1.012*	1.012*	0.903*
0.5	0.814	1.022	0.857	0.715
0.6	0.677	1.035*	0.718*	0.563*

2. Experimental Apparatus

The combustor used for all of the atmospheric pressure measurements in this study is shown to scale in Figure 1. Ultra high purity hydrogen and nitrogen are individually metered from gas cylinders to the fuel tube using separate mass flow controllers. The fuel tubes are made from 1/8" OD stainless steel tubing with varying wall thicknesses, each tapered to a thin lip at the jet exit, with measured jet exit diameters of 0.84 mm, 1.45 mm, and 2.12 mm. Another mass flow controller delivers high purity air to the coflow air apparatus, consisting of a packed bed of copper beads overlaid with a stack of wire mesh screens. In all cases, the coflow air is supplied at an equivalence ratio of $\Phi = 0.5$ or 0.33, and its velocity calculated to be less than 0.25% of the fuel jet velocity.

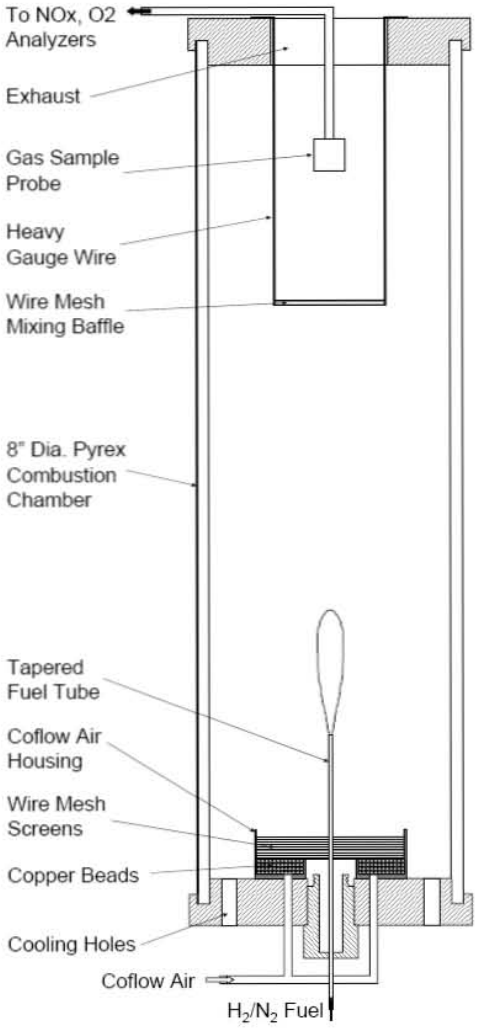

Figure 1: Experimental apparatus for atmospheric pressure NOx measurements

The combustion chamber is made from an 8" Pyrex cylinder whose wall temperature is monitored with externally mounted thermocouples. The cylinder can be internally cooled via ambient air flow through eight ½" holes around the base of the combustion chamber, though these holes were sealed for all experiments in this study, as cooling was deemed unnecessary.

The top of the combustion chamber is fitted with an aluminum cap to direct the exhaust to an overhead vent. To prevent NOx profiles at the exhaust, a mixing baffle composed of three wire mesh screens is suspended from the aluminum cap by three heavy gauge wires. A gas sampling probe draws well-mixed combustion products through a heated sample line to a NOx converter, followed by an ice bath and desiccant trap to remove any water vapor from the gas sample. The gas is then analyzed by Rosemount NGA2000 NOx and oxygen analyzers. Global NOx measurements, $\chi_{NOx,measured}$, are then corrected to 15% oxygen, $\chi_{NOx@15\%O2}$, using the measured oxygen content in the exhaust gas, $\chi_{O2,measured}$, as follows [11]:

$$\chi_{NOx@15\%O2} = \chi_{NOx,measured} \frac{0.21 - 0.15}{0.21 - \chi_{O2,measured}} . \quad (2)$$

Corrected NOx @ 15% O2 can also be converted to an emission index using [11]:

$$EINO_x = \frac{\chi_{NOx@15\%O2}}{1000} \frac{N_{prod@15\%O2}}{N_{H2}} \frac{M_{NO2}}{M_{H2}} , \quad (3)$$

where $N_{prod@15\%O2}/N_{H2}$ is the total moles of dry combustion products containing 15% oxygen, per mole of hydrogen burned, and M_{NO2} and M_{H2} are the molecular weights of NO_2 and H_2,

respectively. Manipulating an atom balance for the combustion of a hydrogen/nitrogen mixture, substitution of an expression for $N_{prod@15\%O2}/N_{H2}$ and the appropriate molecular weights yields:

$$EINO_x = \chi_{NOx@15\%O2}\left(0.15 + 0.080\begin{matrix} a \\ 1-a \end{matrix}\right) \quad \left[\begin{matrix} g\,\mathrm{NO_2} \\ kg\,\mathrm{H_2} \end{matrix}\right] \tag{4}$$

where a is the nitrogen diluent fraction in the fuel mixture.

Experiments were performed on each of the three fuel jet diameters, with hydrogen diluted by 10% to 60% nitrogen. Jet exit velocities were varied from 40% to 95 or 98% of the blowoff velocity for each combination of jet exit diameter and nitrogen diluent fraction. Flame lengths are averaged over three visual measurements by a trained observer.

High pressure experiments were performed in NETL's SimVal combustor, an optically accessible, high-pressure combustor designed for studies on lean-premixed flames, which was modified to accommodate the dilute diffusion injection geometry. These experiments were run at 2, 4 and 8 atm using 40% and 50% nitrogen in hydrogen as the fuel. In all cases, the fuel tube used had a jet diameter of 4.57 mm and a blunt tip, and air was delivered at an equivalence ratio of $\Phi = 0.3$, corresponding to 2.9% of the jet exit velocity. More details on this facility can be found in Ref. 12. The main difference between the combustor geometry for the high-pressure and atmospheric pressure experiments is the higher air velocity relative to the fuel jet velocity for the high-pressure combustor. The higher air velocity was still low compared to the fuel jet velocity and was not believed to have a major impact on flame characteristics or NOx formation.

3. Results and Discussion of Atmospheric Pressure Experiments

The effect of increasing nitrogen dilution on flame length is shown the flame photos of Figure 2, where a ten second exposure time was used to enhance flame visibility. Increasing the nitrogen content of the fuel jet both increases the jet density, which entrains more air into the flame, and displaces hydrogen in the fuel jet, thus requiring less air to burn all of the fuel. Both effects serve to decrease the flame length, and are consistent with jet flame length scaling laws for momentum-dominated flames. These scaling laws dictate that the flame length should be independent of jet exit velocity and proportional to the momentum-weighted jet diameter. In some studies, the momentum-weighted jet diameter is based on the ratio of jet to flame product densities [13, 14], though the current flame length data achieves better collapse and agreement with the theory of Delichatsios [15], where the ambient density is used in place of the flame density in the momentum-weighted jet diameter. Factoring in the effects of stoichiometry, the visual flame length can be expressed as $L_f = cd_0^*/f_s$, where f_s is a stoichiometric mixture fraction, and c is a proportionality constant (or dimensionless flame length), set equal to 23 in Ref 15.

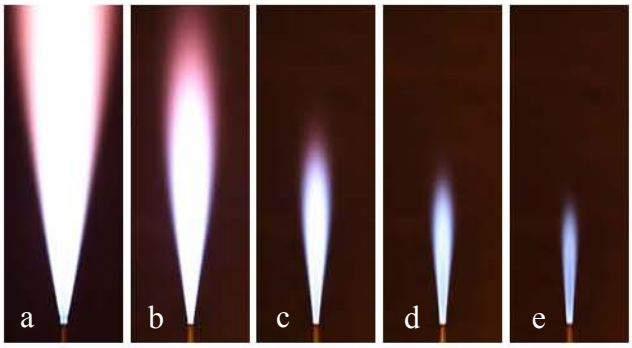

Figure 2: Effect of nitrogen dilution on flame length. Hydrogen with: a) 0% N_2, b) 20% N_2, c) 40% N_2, d) 50% N_2, and e) 60% N_2.

Dimensionless flame lengths for all flames with 30 to 60% nitrogen dilution and jet diameters of 0.84 and 1.45 mm are shown in Figure 3, where laminar flames that do not fit within the fully-developed turbulent jet flame theory are easily distinguished as having dimensionless flame lengths larger than the theoretical value of 23. While the remaining dimensionless flame lengths are smaller than this theoretical limit, this is most likely due to a more conservative definition of the visual flame height in this work. The relatively small scatter (~±7%) about the dimensionless flame height of 20 indicates that the measurements are accurate and repeatable, and that the fully developed turbulent flames follow the proper scaling laws.

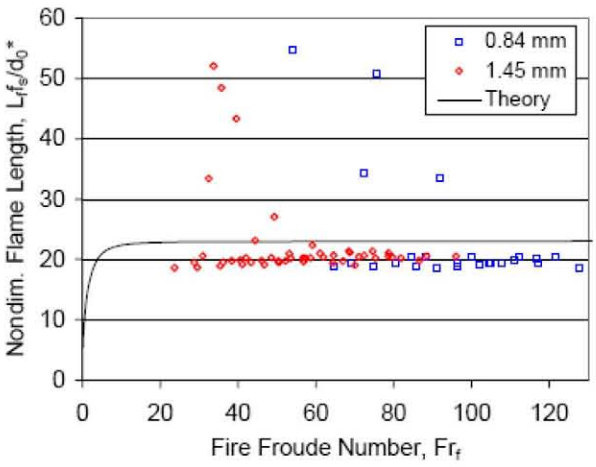

Figure 3: Corrected global NOx emission vs. jet exit Reynolds number

Although the flame length measurements are accurate to about ± 1/16", up to 16% error in the residence time can occur for the smallest flame lengths (1¼") due to the cubic dependence of residence time on flame length. As a result, flame lengths used in residence time calculations below are either averages of all measured turbulent flame lengths for a particular jet diameter and nitrogen diluent fraction, or are computed using $c = 20$ as a dimensionless flame length.

The effects of flame length and turbulence on NOx can be seen in Figure 4, which shows the dependence of the global NOx emissions, corrected to 15% O2, on the jet exit Reynolds number for the 0.84 and 1.45 mm jet diameters. For Re < 2400, the flames give a laminar appearance and are very long compared to their turbulent counterparts. The extended flame lengths and low jet exit velocities produce long flame residence times and result in increased thermal NO generation. For jet exit Reynolds numbers above 2400 and below about 2800, the flames appear in a transitional state, with laminar bases and turbulent tips. With flame lengths in between those of laminar and fully turbulent flames, these transitional flames also produce higher NOx than the fully turbulent flames, and are excluded in subsequent figures. The upper boundary of this transitional regime is not clearly defined, and may have a slight dependence on jet diameter, as the normalized EINOx measurements below would seem to indicate.

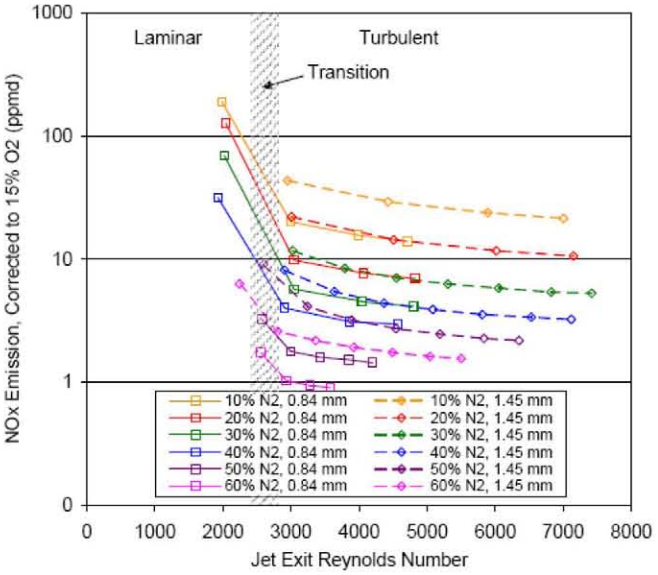

Figure 4: Global NOx measurements vs. jet Reynolds number for 0.84 & 1.45 mm jets.

In Figure 5, the global NOx, corrected to 15% O_2, is plotted against jet exit velocity for all jet diameters and nitrogen diluent fractions used in this study. The data show the expected trends: decreasing NOx emission for smaller jet diameters, higher jet velocities, and increasing nitrogen diluent in the fuel jet. It is noteworthy that for a 50/50 mixture of hydrogen and nitrogen, the target fuel for the FutureGen program, the 0.84 mm jet diameter achieved a low of about 1.4 ppm NOx, though higher NOx emissions would naturally be expected at gas turbine conditions.

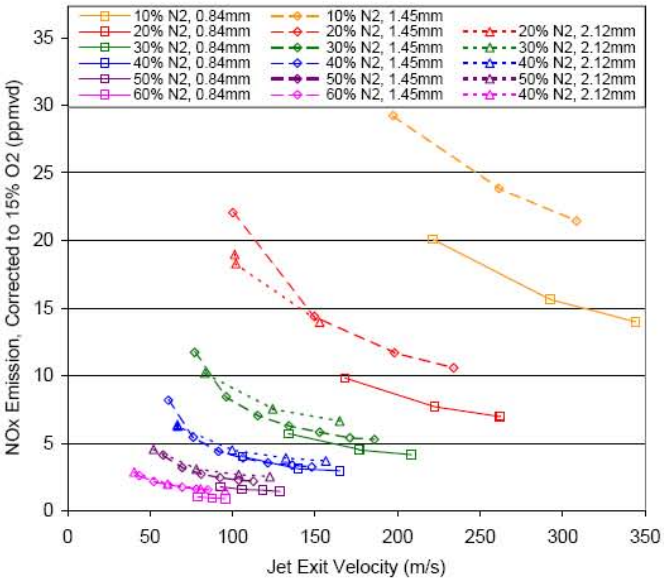

Figure 5: Corrected global NOx measurements vs. jet exit velocity for all jet diameters and nitrogen diluent fractions

Converting the global NOx emissions in Figure 5 to emission indices by using Eq. (4) and normalizing by the residence time, τ_r, the results are plotted against the global strain rate, u_0/d_0^*, in Figure 6. For each jet diameter and nitrogen dilution, the results show that higher strain rates approach the ½ power slope that has been observed in other studies, indicative of turbulence-chemistry interactions in the flame [5–9]. For a given nitrogen dilution, results from different jet exit diameters fall on roughly the same line, with flame length measurement errors likely resulting in any deviations. In addition, Figure 6 shows that the effect of flame strain is similar for different nitrogen dilutions and is primarily due to reductions in flame lengths and residence times. Any flame temperature reductions that might be expected by diluting the hydrogen fuel with nitrogen are effectively offset both by decreasing the fuel Lewis number, which serves to increase peak flame temperatures [9], and by increased thermal NO production due to increased N2 concentrations in the high temperature regions of the flame [4].

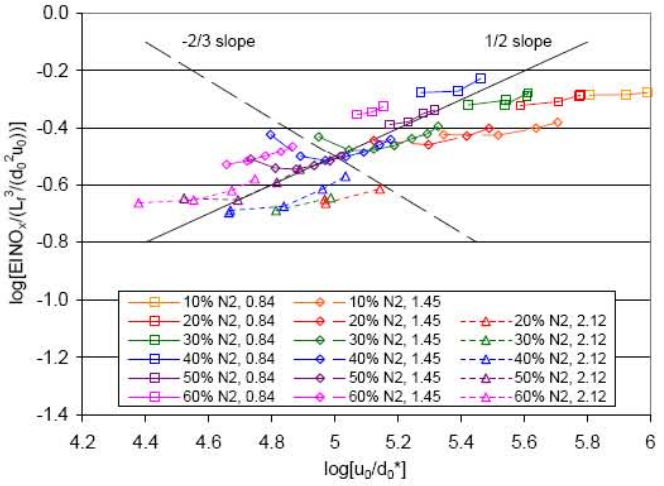

Figure 6: Log of EINOx normalized by flame residence time vs. log of global flame strain

For lower global strain rates, it is observed that the normalized emission index departs from the 1/2 power slope (n = -1/2), trending towards a zero slope (n = 0), and, in the case of the 1.45 mm jet diameter, progressing towards the -2/3 slope (n = 2/3) observed by Gabriel et. al. [9]. The reason for departure from the 1/2 power slope may be due to a reduction in turbulence-chemistry interactions and an approach towards equilibrium chemistry, however, it may also be a function of the degree of initial turbulence at the jet exit. The log of the normalized emission index is

plotted against the Reynolds number in Figure 7, where it can be seen that the normalized emission index reaches a minimum at a Reynolds number of about 4400 for the 1.45 mm jet diameter. Increasing NOx for $Re < 4400$ may be due to laminar structures present in the flame, which have been observed up to $Re \approx 4000$ in hydrogen jet flames diluted with 50% nitrogen [16]. Additional data needs to be taken in this range for the 2.12 mm jet diameter to confirm that these trends are the result of Reynolds number effects, although data from the 0.84 mm jet diameter and data from other studies do not support this claim. Additional study will be required to determine the cause of the trends indicated by the 1.45 mm jet diameter data.

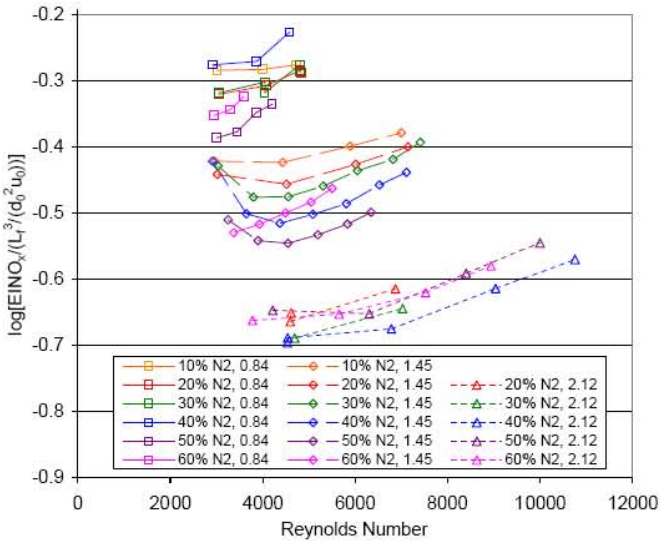

Figure 7: log of emission index normalized by flame residence time vs. Reynolds number for all flames

Finally, the results of Figure 6 do not indicate that the slope of the normalized EINOx with respect to global strain varies for a particular level of dilution, as has been suggested by Gabriel et. al. [9]. The change in slope from 1/2 to -2/3 was observed for 60% Ar and 60% CO_2 dilution, and was presumably linked to the fuel Lewis numbers shown in Table 1 [9]. Given that Le_F for 60% N_2 falls between those for 60% Ar and 60% CO_2 dilution, it was expected that the same -2/3 slope might also occur for this level of nitrogen dilution, and possibly for a dilution level of 50% nitrogen as well. The results of this study indicate that this is not the case, since the 60% nitrogen dilution cases all approach the 1/2 power slope at high strain rates.

4. Results and Discussion of High-Pressure Experiments

NOx measurements in the high-pressure combustor were made at 2, 4 and 8 atm with fuels containing 40% and 50% nitrogen dilution by volume with the balance being hydrogen. Due to the design of the gas sampling system, measurements at 1 atm were not possible, therefore it is difficult to make direct comparisons to the atmospheric pressure data above. For each condition, the fuel and air flowrates were ramped up at constant equivalence ratio and pressure until the flame was visibly lifted from the tip of the fuel tube. Each ramp lasted about 20 minutes and NOx measurements in the exhaust gas stream were made every second.

Figure 8 is a plot of NOx verses jet velocity for both nitrogen dilutions at all three pressures. The data follow the same trend with respect to jet velocity as was observed in the atmospheric pressure experiments. NOx was found to increase significantly with pressure, which was attributed to an increase in reaction rates as pressure was increased. The effect of increasing the reaction rates relative to strain rate can be understood through a Damköhler number. Although visual flame length measurements were not made due to fouling of the combustor liner and low flame luminosity, the theoretical flame length can be deduced from the scaling law ($L_f = cd_0^*/f_s$,) and should be independent of pressure. Global strain rate and flame residence time can be also

be argued to be independent of pressure, but the effect of local strain rate and thus departure from equilibrium conditions can be related to the Damköhler number ($Da = \tau_t / \tau_c$) where τ_t is the turbulent mixing timescale and τ_c is the chemical timescale. The effect of Damköhler number on emission index has been observed by Chen and Driscoll [5] and is accounted for in Eq. 1. As pressure and thus reaction rates are increased, the Damköhler number increases and NOx formation goes up as well. In the limit of infinitely high pressure, temperature and species concentrations in the flame should approach equilibrium values. The net effect is that increasing the pressure reduces the effect of local flame strain on suppressing NOx formation.

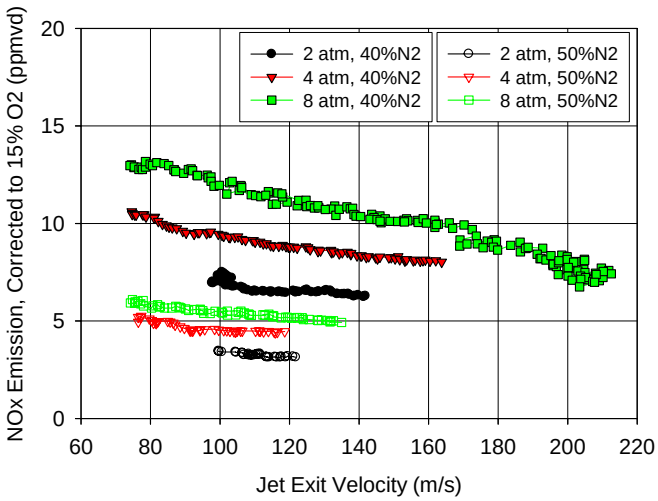

Figure 8: Corrected global NOx measurements vs. jet exit velocity for high-pressure experiments (Dj=4.57 mm).

The effect of pressure on NOx emissions was found to be dependent on nitrogen dilution in the fuel with a secondary dependence on jet velocity. Averaging over all velocities, NOx emission was found to scale with pressure to the 0.38 power for the 40% nitrogen dilution and pressure to the 0.32 power for the 50% nitrogen dilution. The dependence on pressure is expected to be a complex function of radical concentrations in the flame, especially O-atoms, which decrease in mole fraction due to three-body recombination reactions as pressure is increased, and flame temperature which is a function of both nitrogen dilution and pressure [17].

Calculations of peak flame temperature and NO concentration using the Chemkin computer package with the OPPDIF code are presented in Figure 9. The calculations were performed using the hydrogen parent mechanism of Li *et al.* [18] and a subset of the GRI3.0 nitrogen chemistry including the thermal, N_2O and NNH routes of NOx formation. Full, multi-component diffusion was used and a constant strain rate of 7000 s^{-1} and nitrogen dilution of 40% was used for the calculations. Fig. 9 clearly shows a strong increase in peak flame temperature as well as NO concentration as pressure is increased at a constant strain rate. The adiabatic flame temperature for the 40% nitrogen dilution fuel was calculated to be 2145K while the flame calculations shown in Fig. 9 show flame temperatures well above this for the higher pressure cases. This is a result of preferential diffusion of the lighter species (H and H_2), and is reflective of a low Lewis number fuel.

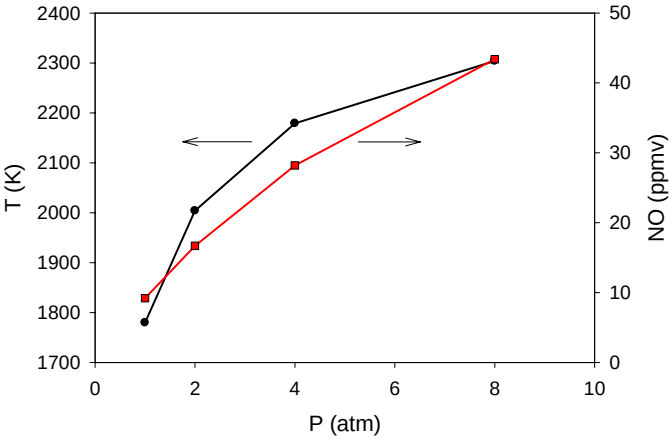

Figure 9: Peak flame temperature and NO concentration calculated with OPPDIF for 40% nitrogen dilution, and strain rate=7000 s-1.

The NOx dependency on pressure is overpredicted with the simple flame calculations shown on Fig. 9 but is useful in understanding the trends observed with operating pressure.

Converting the NOx measurements to emission index and normalizing by flame residence time, as was done with the atmospheric pressure data, results in a similar trend with the data closely following the ½ power slope as shown in Figure 10. Theoretical flame lengths were calculated to be 297 mm for the 40% nitrogen dilution and 252 mm for the 50% nitrogen dilution. As was observed in the atmospheric pressure measurements, the effect of nitrogen dilution on normalized emission index is very small, indicating that the expected decrease in flame temperature with increasing nitrogen dilution is offset by the decrease in fuel Lewis number, which serves to increase the flame temperature through preferential diffusion. Since Lewis number is independent of pressure, an increase in normalized emission index with increasing pressure is observed as a variation in the data in the vertical direction in Fig. 10, and is due to the increase in reaction rates and peak flame temperature, which can be related to an increase in Damköhler number.

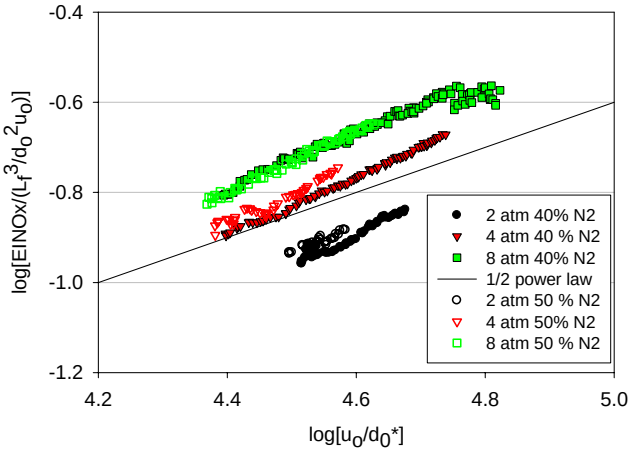

Figure 10: log of EINOx normalized by flame residence time vs. log of global strain rate for high-pressure experiments (Dj=4.57 mm).

5. Conclusions

The conclusions of this study can be summarized as follows:

1. The residence time-normalized emission index plotted against the global strain rate exhibits a 1/2 power slope at high strain rates, as observed in other studies [5–9].
2. For flames with a jet exit Reynolds number near the laminar-turbulent transitional regime, the slope of the normalized emission index decreases to zero and in some cases becomes negative, presumably due to the existence of laminar structures in these flames.
3. The slope of the normalized emission index was found to be insensitive to the Lewis number of the fuel mixture in the fully turbulent regime, which is in disagreement with the results of other studies [9].
4. The expected decrease in flame temperature with increasing nitrogen dilution was offset by the decrease in fuel Lewis number, which increases the peak flame temperature through preferential diffusion. The result is that the emission index, normalized by flame residence time, is largely insensitive to nitrogen dilution, and any emissions reductions that can be achieved through nitrogen dilution are attained solely through reductions in the flame length and residence time.
5. NOx emissions were found to increase with operating pressure due to an increase in reaction rates and peak flame temperatures. The ½ power slope was found to be valid for

the high-pressure results. The effect of nitrogen dilution on reducing NOx emissions was attained through a reduction in flame length and residence time, as was observed in the atmospheric pressure measurements.

The implication of the above study for NOx reduction in a high-pressure gas turbine combustor is that higher velocities and lower residence times would need to be reached relative to those studied here in order to achieve NOx levels in line with DOE program goals. This could most easily be achieved by using an array of small, low-residence time jets rather than a single jet in a high pressure combustor. An additional pathway to lower NOx diffusion flames may lie in the use of high coaxial air velocities, as they are expected to reduce flame lengths, residence times and strain rates simultaneously, thereby resulting in lower thermal NOx.

Acknowledgements

The authors would like to thank Fred White for his assistance in the setup of the atmospheric pressure combustor, and Todd Sidwell and Mark Tucker for their contributions to the operation of the high pressure combustor facility. The support of the U.S. DOE Turbines program is also gratefully acknowledged.

References

[1] Todd, D. M., and Battista, R. A., "Demonstrated Applicability of Hydrogen Fuel for Gas Turbines," Proceedings of the IChemE "Gasification 4 the Future" Conference, Noordwijk, the Netherlands, April 11-13, 2000.
[2] Drake, M. C., Correa, S. M., Pitz, R. W., Shyy, W., and Fenimore, C. P., *Combust. Flame*, 69:347-365, (1987).
[3] Sanders, J. P. H., Chen, J.-Y. and Gökalp, I., *Combust. Flame*, 111:1-15, (1997).
[4] Turns, S. R., *Progress En. Combust. Sci.*, 21:361- , (1995).
[5] Chen, R.-H., and Driscoll, J. F., *Twenty-Third Symposium (International) on Combustion*, The Combustion Institute, Pittsburgh, 281-288, (1990).
[6] Driscoll, J. F., Chen, R.-H., and Yoon, Y., *Combust. Flame*, 88:37-49, (1992).
[7] Chen, J.-Y., and Kollmann, W., *Combust. Flame*, 88:397-412, (1992).
[8] Smith, N. S. A., Bilger, R. W., and Chen, J.-Y., *Twenty-Fourth Symposium (International) on Combustion*, The Combustion Institute, Pittsburgh, 33-42, (1981)..
[9] Gabriel, R., Navedo, J. E., and Chen, R.-H., *Combust. Flame*, 121:525-534, (2000).
[10] Chao, Y.-C., Wu, C.-Y., Lee, K.-Y., Li, Y.-H., Chen, R.-H., and Cheng, T.-S., *Combust. Sci. and Tech.*, 176: 1735-1753, (2004).
[11] Turns, S. R., *An Introduction to Combustion: Concepts and Applications*, 1st Ed., McGraw-Hill, New York, 1996.
[12] Sidwell, T., Richards, G., Casleton, K., Straub, D., Maloney, D., Strakey, P., Ferguson, D., Beer, S., and Woodruff, S., *AIAA*, 44(3):434-443, (2006).
[13] Becker, H. A., and Liang, D., *Combust. Flame*, 32:115-137, (1978).
[14] Blake, T. R., and McDonald, M., *Combust. Flame*, 101:175-184, (1995).
[15] Delichatsios, M. A., *Combust. Flame*, 92:349-364, (1993).
[16] Takahashi, F., Mizomoto, M., and Ikai, S., *Combust. Flame*, 48:85-95, (1982).
[17] Correa, S. M., *Combust. Sci. and Tech.*, 87:329-362, (1992).
[18] Li, J., Zhao, Z., Kazakov, A., and Dryer, F., *Int. J. Chem. Kinetics*, 36:1-10, (2004).